

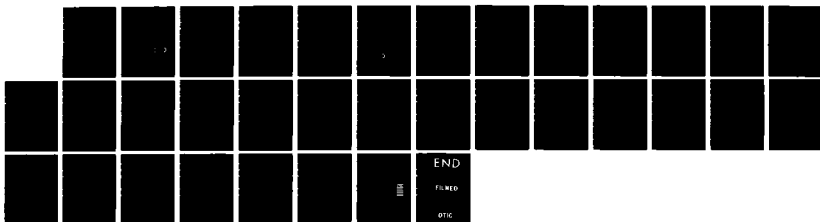
AD-A153 693

INVESTIGATION OF SEVERAL LOW-LYING LEVELS OF X DOUBLET
PT STATE OF NCO US. (U) ARMY BALLISTIC RESEARCH LAB
ABERDEEN PROVING GROUND MD W R ANDERSON ET AL DEC 84
BRL-TR-2625 SBI-AD-F300 592 F/G 21/2

1/1

UNCLASSIFIED

NL



B
R
L

AD-A153 693

AD

2

TECHNICAL REPORT BRL-TR-2625

INVESTIGATION OF SEVERAL LOW-LYING
LEVELS OF X DOUBLET PI STATE OF NCO
USING ARGON LASER EXCITED FLUORESCENCE

Koon Ng Wong
William R. Anderson
Anthony J. Kotlar
John A. Vanderhoff

December 1984

DTIC
ELECTE
APR 5 1985
S D
B

APPROVED FOR PUBLIC RELEASE; DISTRIBUTION UNLIMITED.

US ARMY BALLISTIC RESEARCH LABORATORY
ABERDEEN PROVING GROUND, MARYLAND

Destroy this report when it is no longer needed.
Do not return it to the originator.

Additional copies of this report may be obtained
from the National Technical Information Service,
U. S. Department of Commerce, Springfield, Virginia
22161.

The findings in this report are not to be construed as an official
Department of the Army position, unless so designated by other
authorized documents.

The use of trade names or manufacturers' names in this report
does not constitute indorsement of any commercial product.

UNCLASSIFIED

SECURITY CLASSIFICATION OF THIS PAGE (When Data Entered)

REPORT DOCUMENTATION PAGE		READ INSTRUCTIONS BEFORE COMPLETING FORM
1. REPORT NUMBER TECHNICAL REPORT BRL-TR-2625	2. GOVT ACCESSION NO. AD A153 673	3. RECIPIENT'S CATALOG NUMBER
4. TITLE (and Subtitle) INVESTIGATION OF SEVERAL LOW-LYING LEVELS OF X DOUBLET PI STATE OF NCO USING ARGON EXCITED FLUORESCENCE LASER		5. TYPE OF REPORT & PERIOD COVERED Final
7. AUTHOR(s) Koon Ng Wong*, William R. Anderson, Anthony J. Kotlar, John A. Vanderhoff		6. PERFORMING ORG. REPORT NUMBER
9. PERFORMING ORGANIZATION NAME AND ADDRESS US Army Ballistic Research Laboratory ATTN: AMXBR-IBD Aberdeen Proving Ground, MD 21005-5066		8. CONTRACT OR GRANT NUMBER(s)
11. CONTROLLING OFFICE NAME AND ADDRESS US Army Ballistic Research Laboratory ATTN: AMXBR-OD-ST Aberdeen Proving Ground, MD 21005-5066		10. PROGRAM ELEMENT PROJECT, TASK AREA & WORK UNIT NUMBER 1L161102AH43
14. MONITORING AGENCY NAME & ADDRESS (if different from Controlling Office)		12. REPORT DATE December 1984
		13. NUMBER OF PAGES 33
		15. SECURITY CLASS. (if this report) Unclassified
		15a. DECLASSIFICATION/DOWNGRADING SCHEDULE NA
16. DISTRIBUTION STATEMENT (of this Report) Approved for public release; distribution is unlimited.		
17. DISTRIBUTION STATEMENT (of the abstract entered in Block 20, if different from Report)		
18. SUPPLEMENTARY NOTES *NAS-NRC Postdoctoral Research Associate Published in Journal of Chemical Physics		
19. KEY WORDS (Continue on reverse side if necessary and identify by block number) NCO Radical Laser Excited Fluorescence Molecular Constants Vibrational Levels		
20. ABSTRACT (Continue on reverse side if necessary and identify by block number) meg The laser excited fluorescence spectrum of NCO from an atmospheric pressure $\text{CH}_4/\text{N}_2\text{O}/\text{N}_2$ flame is reinvestigated with a more sensitive apparatus than used previously. The NCO is pumped from the X doublet pi (1,0,0) level to the A doublet sigma plus (0,0,0) level. Emissions from the excited A state level to the following X state vibrational levels are observed: doublet pi (0,0,0), (1,0,0), and (0,0,1); doublet sigma plus (0,1,0). The previous tentative assignment of pumping transition as Q2(31) is confirmed. The confirmation		

UNCLASSIFIED

SECURITY CLASSIFICATION OF THIS PAGE (When Data Entered)

of pumping transition solidifies our earlier interpretation that excited state spin relaxation in the flame is much faster than electronic quenching. In addition, analysis of the fluorescence spectra yields the first reported constants for the X doublet π (1,0,0) level and spin splitting for the X doublet π (0,0,1) level in the gas phase.

UNCLASSIFIED

SECURITY CLASSIFICATION OF THIS PAGE (When Data Entered)

TABLE OF CONTENTS

	<u>Page</u>
I. INTRODUCTION.....	5
II. EXPERIMENTAL DETAILS.....	7
III. RESULTS AND DISCUSSION.....	11
IV. CONCLUSIONS.....	17
ACKNOWLEDGEMENTS.....	19
REFERENCES.....	20
APPENDIX A.....	23
DISTRIBUTION LIST.....	27

DTIC
ELECTE
S APR 5 1985 **D**
B

Approved For	
DTIC	<input checked="" type="checkbox"/>
Excluded	<input type="checkbox"/>
Classification	<input type="checkbox"/>
Distribution/	
Availability Code	
Avail and/or	
Special	
Dist	
A-1	



I. INTRODUCTION

Recently we reported the laser excited fluorescence (LEF) spectra from the A-X system of the free NCO radical in a rich atmospheric pressure $\text{CH}_4/\text{N}_2\text{O}/\text{N}_2$ flame using a fixed wavelength argon ion laser.¹ NCO is of interest because thermal decomposition studies of various gun propellants have shown that HCN is formed as one of the decomposition products.² Shock tube studies of the oxidation of HCN indicate that NCO is an important intermediate in the further reaction of HCN.³ All nine lines (4545 to 5145 Å) of the argon ion laser pump vibrational bands of the $\text{A}^2\Sigma^+ - \text{X}^2\Pi$ electronic system. The 4658 Å pump line was selected for detailed study because it pumps directly to the $\text{A}^2\Sigma^+ (0,0^0,0)$ level. (See the Appendix for a short explanation of the terminology used for vibrational levels.) Since no vibrational down-transfer in the excited state can occur, the resulting fluorescence spectra are simpler than for the other pump lines. In addition, though this is one of the weakest laser lines, the fluorescence from this pump line is the strongest.¹ This is probably because the line pumps from one of the lowest vibrational levels, $\text{X}^2\Pi (1,0^1,0)$, while the other lines pump from higher levels. It was firmly established in Ref. 1 that NCO is pumped to $\text{N}'=31$ by this line. However, the lower rotational level (N'' , J'') from which pumping occurs has not been confirmed due to C_2 and grating ghost interferences in the region of the laser line. In addition, emission to the $(0,0^1,1)$ vibrational level of the $\text{X}^2\Pi$ ground electronic state was not observed because of the deterioration of the laser power in the later part of the study.

The A-X system of NCO was first observed in low resolution emission spectra by Holland, et al.⁴ An extensive vibrational and rotational analysis of this electronic system was performed by Dixon.⁵ Bolman, et al.,⁶

¹W.R. Anderson, J.A. Vanderhoff, A.J. Kotlar, M.A. DeWilde, and R.A. Beyer, "Intracavity Laser Excitation of NCO Fluorescence in an Atmospheric Pressure Flame," BRL Technical Report ARBRL-TR-02527, September 1983, A134740.

²(a) R.A. Beyer, "Molecular Beam Sampling Mass Spectrometry of High Heating Rate Pyrolysis: Description of Data Acquisition System and Pyrolysis of HMX in a Polyurethane Binder," BRL Memorandum Report ARBRL-MR-02816, 1978, A054328. (b) C.U. Morgan and R.A. Beyer, "ESR and IR Spectroscopic Studies of HMX and RDX Thermal Decomposition," 15th JANNAF Combustion Meeting, Newport, RI, September 1978.

³R.A. Fifer and H.E. Holmes, "Kinetics of the $\text{HCN} + \text{NO}_2$ Reaction Behind Shock Waves," J. Phys. Chem., Vol. 86, p. 2935, 1982.

⁴R. Holland, D.W.G. Style, R.N. Dixon, and D.A. Ramsay, "Emission and Absorption Spectra of NCO and NCS," Nature (London), Vol. 182, p. 336, 1958.

⁵R.N. Dixon, "The Absorption Spectrum of the Free NCO Radical," Phil. Trans. R. Soc. London, Vol. 252, p. 165, 1960.

⁶P.S.H. Bolman, J.M. Brown, A. Carrington, I. Kopp, and D.A. Ramsay, "A Re-Investigation of the $\text{A}^2\Sigma^+ - \text{X}^2\Pi$ Band System of NCO," Proc. R. Soc. London Ser. A, Vol. 343, p. 17, 1975.

reinvestigated the A-X system at higher resolution. The free NCO radical has also been studied by electron paramagnetic resonance⁷ and by microwave spectroscopy.^{8,9} These investigations provide much information concerning the upper state, the ground state, and its associated bending vibrational levels. However, there is little information available on the two stretching vibrations of the $X^2\Pi$ ground electronic state. Using the matrix isolation technique, Milligan and Jacox¹⁰ were able to obtain values of the two stretching frequencies, which were confirmed later by Bondybey and English¹¹ in their study of the LEF spectra of NCO in an argon matrix. Recently Barnes, et al.,¹² obtained spectroscopic parameters in the $(0,0^1,1)$ vibrational level of the $X^2\Pi$ state by using CO laser magnetic resonance.

For the reasons mentioned above, we reinvestigated the LEF spectra of NCO using the 4658Å pump line when the argon ion laser was in a good working condition. (A new, higher power tube was installed). All emissions from the $A^2\Sigma^+ (0,0^0,0)$ level to the ground state levels observed in the argon matrix work,¹¹ i.e., $(0,0^1,0)^2\Pi$, $(1,0^1,0)^2\Pi$, $(0,1^0,0)^2\Sigma^+$, and $(0,0^1,1)^2\Pi$, have been observed.* The C_2 interferences in the $(1,0^1,0)$ band have been minimized (vide infra) and our tentative assignment that Q_{231} is the pumping transition has been confirmed. Furthermore, these higher S/N spectra allow analyses of the $(0,0^1,0)$, $(1,0^1,0)$, and $(0,0^1,1)$ emission bands yielding values for the two stretching vibrational frequencies, the rotational constants, and the

⁷A. Carrington, A.R. Fabris, B.J. Howard, and N.J.D. Lucas, "Electron Resonance Studies of the Renner Effect. I. Gaseous NCO In Its $^2\Pi_{3/2}$ ($n=1$), $^2\Pi_{5/2}$ ($n=2$), and $^2\Pi_{7/2}$ ($n=3$) Vibronic States," Mol. Phys., Vol. 20, p. 961, 1971.

⁸S. Saito and T. Amano, "Microwave Spectrum of the NCO Radical," J. Mol. Spectrosc., Vol. 34, p. 383, 1970.

⁹T. Amano and E. Hirota, "Hyperfine Interactions of the Free NCO Radical in the A Vibronic State ($v_2=1$)," J. Chem. Phys., Vol. 57, p. 5608, 1972.

¹⁰D.E. Milligan and M.E. Jacox, "Matrix Isolation Study of the Infrared and Ultraviolet Spectra of the Free Radical NCO," J. Chem. Phys., Vol. 47, p. 5157, 1967.

¹¹V.E. Bondybey and J.H. English, "Fermi Resonance and Vibrational Relaxation in the $A^2\Sigma^+$ State of NCO in Solid Argon," J. Chem. Phys., Vol. 67, p. 2868, 1977.

¹²C.E. Barnes, L.M. Brown, A.D. Fackerell, and T.J. Sears, "The Laser Magnetic Resonance Spectrum of the NCO Radical at 5.2 μ m," J. Mol. Spectrosc., Vol. 92, p. 485, 1982.

*For the sake of convenience, we will refer to them as the $(0,0^1,0)$, $(1,0^1,0)$, $(0,1^0,0)$, and $(0,0^1,1)$ emission bands from hereon.

spin-orbit coupling constants in all these levels. The $(1,0^1,0)$ band has not been reported previously in gaseous phase. The results are compared to those from the earlier studies mentioned above and also to the preliminary results of a concurrent LEF study.¹³ Excellent agreement is observed.

II. EXPERIMENTAL DETAILS

The experimental arrangement is similar to that described earlier,¹ and only a brief description will be given here. A nominal 8 W (all lines) Ar^+ laser was used as the excitation source. The 4658 Å line, which has a power of about 0.5 W, was selected for this study. A knife-edge burner¹⁴ supporting a $\text{CH}_4/\text{N}_2\text{O}/\text{N}_2$ flame was placed inside the extended cavity of the laser. The intracavity circulating power was approximately 20 times more intense than the extracavity power (i.e., 10 W). The burner was placed in a horizontal position with the open channel facing the detection optics. The scattered light perpendicular to the beam was imaged onto the 100 μm slit of a 1 m monochromator. A glass dove prism was placed in front of the slit to rotate the image 90°. Instead of a photomultiplier tube with photon counting electronics, as used in our previous work,¹ an optical multichannel analyzer (OMA) with a silicon intensified vidicon tube was used to detect the LEF signal. A laboratory computer (PDP 11/34) directly interfaced to the OMA allows for the averaging of spectra for long time periods. In order to remove flame background emissions, the spectra were recorded with and without the laser, then subtracted to obtain the LEF spectra. The results were obtained with approximate flame conditions of equivalence ratio $\phi = 1.6$ with 40% dilution with N_2 .*

The bands displayed in Figures 1, 2, and 3 are actually made up of two or more sections of the LEF spectra taken at different times. The arrows indicate the locations at which these components are joined together to form the entire band. A section of the entire band was taken with the monochromator set at a certain wavelength. The spectra were taken in second order. Approximately 35 Å of the spectrum was accumulated into the 500 channels of the OMA at any one time. The achieved resolution was about 0.4 Å (1.8 cm^{-1}) FWHM.

¹³(a) R.A. Copeland, D.R. Crosley, and G.P. Smith, "Laser-Induced Fluorescence Spectroscopy of NCO and NH_2 in Atmospheric Pressure Flames," submitted to the 20th Symposium (International) on Combustion, Ann Arbor, MI, August 1984. (b) D.R. Crosley, private communication.

¹⁴R.A. Beyer and M.A. DeWilde, "Simple Burner for Laser Probing of Flames," Rev. Sci. Instrum., Vol. 53, p. 103, 1982. A description of the burner suitable for purposes of understanding the spectroscopy discussed in the present work is contained in Ref. 1.

*Since some confusion has resulted in the past, we should note here that 40% dilution with N_2 means 40% of the premixed gases flowing in the burner's main channel is N_2 . Small additional flows of N_2 at the two ends of the burner are used to keep the flame from curling around the knife edges. These additional flows do not alter conditions at the center of the flame where measurements are taken.

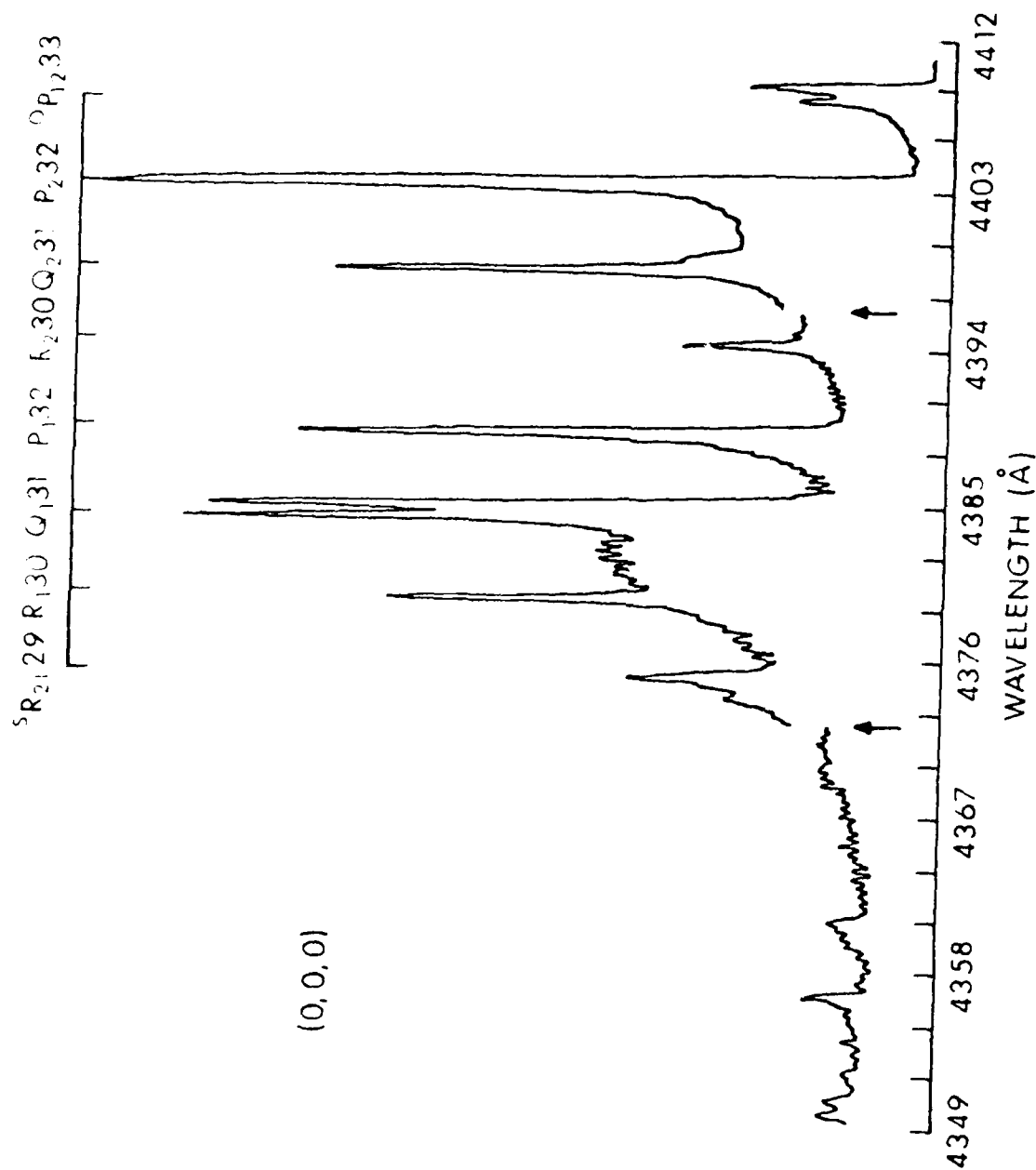


Figure 1. The $A^2\Sigma^+(0,0^0,0) \rightarrow X^2\Pi(0,0^1,0)$ Fluorescence Spectrum. Unlabeled peaks between 4349 and 4367 Å are heads of the $A^2\Pi(0,1^1,0) \rightarrow X^2\Delta(0,1^2,0)$ transition. The upper level is apparently excited via a small amount of vibrational up-transfer from $A^2\Sigma^+(0,0^0,0)$.

$^5R_{21}29$ $R_{13}30$ $Q_{13}31$ $P_{13}32$ $R_{23}30$ $Q_{23}31$ $P_{23}32$ $^5P_{12}33$

(1,0,0)

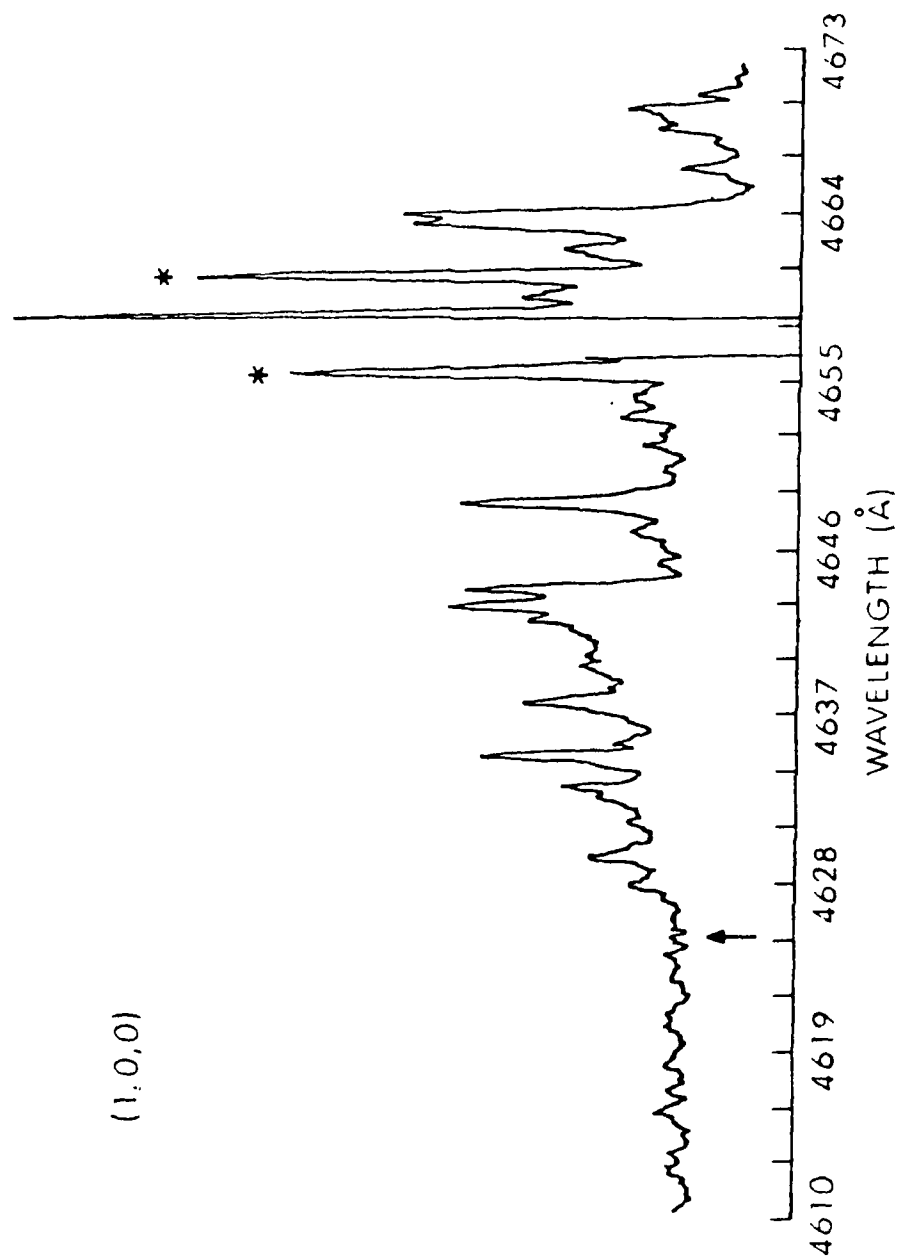


Figure 2. The $A^2\Sigma^+(1,0^0,0) \rightarrow X^2\Pi(1,0^1,0)$ Fluorescence Spectrum. The spectrum drops to zero near 4658 Å because of detection system saturation by laser scatter. The two peaks labeled (*) are grating ghosts.

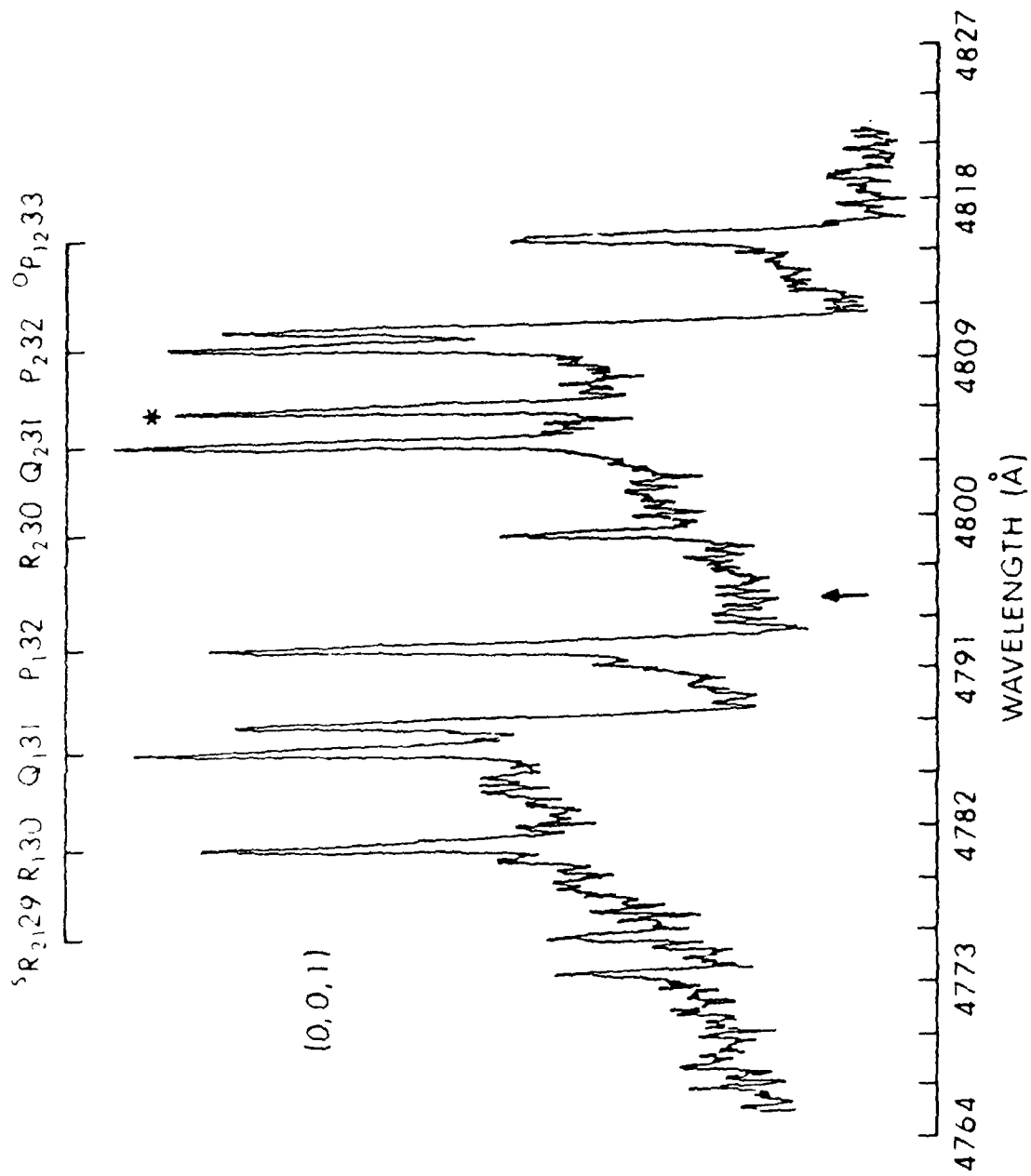


Figure 3. The $A^2\Sigma^+ (0,0^0,0) + X^2\Pi (0,0^1,1)$ Fluorescence Spectrum. The peak at $\sim 4772\text{\AA}$ is unassigned. The peak labeled (*) is an argon discharge line from the laser.

Recording of spectra with the monochromator-OMA system takes much less time than with the earlier photon counting system. A 1000 scan spectrum, for instance, takes about three to four minutes. The increase in number of scans allows for a significant increase in S/N via signal averaging. Another major advantage of the OMA is that it allows one to look at large segments of the spectrum very quickly, often in real time. However, wavelength nonlinearities have been observed across the face of the vidicon tube. These nonlinearities occur because the grating focusses various wavelengths in an arc at the monochromator exit, where the vidicon is placed. Since the vidicon face is flat, the wavelength scale is stretched near the edges. The effect also causes some loss of resolution near the edges of a scan. Fortunately, the mid-section of the spectrum, i.e., from about 100th to 400th channel, is quite linear and gives accurate frequencies (wavelengths). For example, the frequencies of the eight lines determined for the $(0,0^1,0)$ band differ with those of Bolman, et al.,⁶ by less than 1 cm^{-1} , despite the moderate resolution employed in this work. For wavelength calibration, the spectra of Ar discharge lines, obtained by imaging stray light from the laser tube, and of Na emissions from a Na vapor lamp were taken under exactly the same conditions as fluorescence spectra. The wavelengths of the reference lines were taken from the MIT tables.¹⁵

III. RESULTS AND DISCUSSION

As mentioned previously, the 4658Å line of the argon ion laser pumps NCO to the $(0,0^0,0)$ level of the $A^2\Sigma^+$ electronic state. Emissions from $A^2\Sigma^+$ $(0,0^0,0)$ to all of the fundamental vibrational levels of the $X^2\Pi$ ground electronic state were observed. They are shown in Figures 1, 2, 3, and 4, corresponding to the $(0,0^1,0)$, $(1,0^1,0)$, $(0,0^1,1)$, and $(0,1^0,0)$ emission bands, respectively. The relative intensities of these bands agree qualitatively with those observed in a low temperature argon matrix.¹¹ The $(0,0^1,0)$ band is the most intense. Emission bands that involve excitation of the ground state stretching vibrations are stronger than that involving the bending vibration. The $(0,0^1,0)$, $(1,0^1,0)$, and $(0,0^1,1)$ emission bands do not involve the bending mode. Therefore, complications such as ℓ -type doubling and Renner effect are absent. Since these transitions all have the overall symmetry $^2\Sigma^+ \rightarrow ^2\Pi$, it is expected that similar structures be observed in these bands.¹ For a $^2\Sigma^+ \rightarrow ^2\Pi$ transition, there are three main branches and three satellite branches in each subband $^2\Sigma^+ \rightarrow ^2\Pi_{1/2}$ and $^2\Sigma^+ \rightarrow ^2\Pi_{3/2}$. However, since the spin splitting in the upper state is very small,^{5,6} four of these satellite branches coincide with main branches, giving rise to only four distinct branches in each subband. The assignments of these bands are straightforward. They are given in Table 1 and illustrated in Figures 1, 2, and 3. Now, from the previous work on the $(0,0^1,0)$ band, we observed that lines from the directly pumped level $N'=31$ are the most prominent features of the spectra.¹ However, considerable rotational transfer in the excited state occurs, yielding lines from many other N' levels as well. Bandheads (not labeled in the figures), therefore, are also expected to appear in each of the bands just to the long wavelength side (or perhaps overlapping) the Q_1 , P_1 ,

¹⁵Atomic line positions were obtained from G.R. Harrison, Massachusetts Institute of Technology Wavelength Tables, MIT, Cambridge, MA, 1969.

DISTRIBUTION LIST

<u>No. Of Copies</u>	<u>Organization</u>	<u>No. Of Copies</u>	<u>Organization</u>
1	Commander USA Missile Command ATTN: AMSMI-R Redstone Arsenal, AL 35898	1	Commander Naval Air Systems Command ATTN: J. Ramnarace, AIR-54111C Washington, DC 20360
1	Commander USA Missile Command ATTN: AMSMI-YDL Redstone Arsenal, AL 35898	3	Commander Naval Ordnance Station ATTN: C. Irish S. Mitchell P.L. Stang, Code 515 Indian Head, MD 20640
2	Commander USA Missile Command ATTN: AMSMI-RK, D.J. Ifshin Redstone Arsenal, AL 35898	1	Commander Naval Surface Weapons Center ATTN: J.L. East, Jr., G-20 Dahlgren, VA 22448
1	Commander USA Tank Automotive Command ATTN: AMSTA-TSL Warren, MI 48090	2	Commander Naval Surface Weapons Center ATTN: R. Bernecker, R-13 G.B. Wilmot, R-16 Silver Spring, MD 20910
1	Director USA TRADOC Systems Analysis Activity ATTN: ATAA-SL WSMR, NM 88002	4	Commander Naval Weapons Center ATTN: R.L. Derr, Code 389 China Lake, CA 93555
1	Commandant US Army Infantry School ATTN: ATSH-CD-CSO-OR Fort Benning, GA 31905	2	Commander Naval Weapons Center ATTN: Code 3891, T. Boggs K.J. Graham China Lake, CA 93555
1	Commander USA Army Development and Employment Agency ATTN: MODE-TED-SAB Fort Lewis, WA 98433	5	Commander Naval Research Laboratory ATTN: L. Harvey J. McDonald E. Oran J. Shnur R.J. Doyle, Code 6110 Washington, DC 20375
1	Office of Naval Research Department of the Navy ATTN: R.S. Miller, Code 432 800 N. Quincy Street Arlington, VA 22217	1	Commanding Officer Naval Underwater Systems Center Weapons Dept. ATTN: R.S. Lazar/Code 36301 Newport, RI 02840
1	Navy Strategic Systems Project Office ATTN: R.D. Kinert, SP 2731 Washington, DC 20376		

DISTRIBUTION LIST

<u>No. Of Copies</u>	<u>Organization</u>	<u>No. Of Copies</u>	<u>Organization</u>
12	Administrator Defense Technical Info Center ATTN: DTIC-DDA Cameron Station Alexandria, VA 22304-6145	1	Director USA Air Mobility Research and Development Laboratory Ames Research Center Moffett Field, CA 94035
1	HQDA DAMA-ART-M Washington, DC 20310	4	Commander US Army Research Office ATTN: R. Ghirardelli D. Mann R. Singleton R. Shaw Research Triangle Park, NC 27709
1	Commander US Army Materiel Command ATTN: AMCDRA-ST 5001 Eisenhower Avenue Alexandria, VA 22333	1	Commander USA Communications - Electronics Command ATTN: AMSEL-ED Fort Monmouth, NJ 07703
1	Commander Armament R&D Center USA AMCCOM ATTN: SMCAR-TDC Dover, NJ 07801	1	Commander USA Electronics Research and Development Command Technical Support Activity ATTN: DELSD-I Fort Monmouth, NJ 07703
1	Commander Armament R&D Center USA AMCCOM ATTN: SMCAR-TSS Dover, NJ 07801-5001	2	Commander USA AMCCOM, ARDC ATTN: SMCAR-LCA-G, D.S. Downs J.A. Lannon Dover, NJ 07801
1	Commander USA AMCCOM ATTN: SMCAR-ESP-L Rock Island, IL 61299	1	Commander USA AMCCOM, ARDC ATTN: SMCAR-LC, L. Harris Dover, NJ 07801
1	Director Benet Weapons Laboratory Armament R&D Center USA AMCCOM ATTN: SMCAR-LCB-TL Watervliet, NY 12189	1	Commander USA AMCCOM, ARDC ATTN: SMCAR-SCA-T L. Stiefel Dover, NJ 07801
1	Commander USA Aviation Research and Development Command ATTN: AMSAV-E 4300 Goodfellow Blvd. St. Louis, MO 63120		

APPENDIX A.

VIBRATIONAL LEVEL TERMINOLOGY AND THE RENNER-TELLER EFFECT IN LINEAR TRIATOMIC MOLECULES

The vibrational level terminology is discussed in detail elsewhere.* A short explanation of the terminology is given here. The designation of the form (v_1, v_2, v_3) refers to a vibrational level as follows. v_1 and v_3 refer, respectively, to symmetric and antisymmetric stretching vibrational quantum numbers of the molecule. Here, it should be noted that although NCO has no center of inversion symmetry, the NC and CO stretching vibrations are strongly coupled.⁵ Therefore, the vibrational stretching motions are similar to those of CO₂. It is thus proper to use the terms symmetric and antisymmetric in reference to the stretching motions in NCO. v_2 refers to the quantum number of the doubly degenerate bending mode. For such degenerate vibrations, the molecule possesses a quantized vibrational angular momentum designated by quantum number, ℓ . ℓ has possible values $v_2, v_2-2, \dots, 1$ or 0 . In the case of linear molecules for which Λ , the electronic orbital angular momentum quantum number is well-defined, ℓ and Λ add vectorially to yield a new quantum number K which takes on all possible values of $|\pm\Lambda \pm \ell|$. Note that K is the superscript on the v_2 quantum number in the vibrational level designation. The value of K determines the overall symmetry (electronic \times vibrational) of the state, i.e., $K = 0, 1, 2, 3 \dots$ corresponds to $\Sigma, \Pi, \Delta, \Phi \dots$ states, respectively. Here, Σ levels are singly and $\Pi, \Delta, \Phi \dots$ levels doubly degenerate, as usual. Now, for $v_2 = 0$, we must have $\ell=0$ so that $K=\Lambda$ and only one vibrational state results. Thus, for $A^2\Sigma^+$ (where $\Lambda=0$) and $X^2\Pi$ (where $\Lambda=1$) $v_2 = 0$ can yield only a $^2\Sigma^+$ and a $^2\Pi$ vibrational level, respectively. For $v_2 > 0$, ℓ may take on values greater than 0 and several states will result. The energies of these states will differ because the bending vibration destroys the cylindrical symmetry of the molecule, removing their degeneracy. This effect is known as the Renner-Teller effect. As an example of interest in the present paper, consider the value $v_2 = 1$ in the $X^2\Pi$ electronic state. Since $v_2 = 1$, ℓ must equal 1 . For the $X^2\Pi$ state, $\Lambda=1$. Thus, the sum rule $K = |\pm\Lambda \pm \ell|$ results in four values, $2, 2, 0$, and 0 . Of these, the two levels with $K=2$ will be equal in energy, yielding a single, doubly degenerate Δ state. The two $K=0$ values will have unequal energies yielding a Σ^+ and a Σ^- state. Therefore, if we consider the $(0,1,0)$ level in the $X^2\Pi$ state, this level will actually be split into three levels, namely, $X^2\Delta(0,1^2,0)$, $X^2\Sigma^-(0,1^0,0)$, and $X^2\Sigma^+(0,1^0,0)$. Dipole radiation selection rules only allow $\Delta K=0, \pm 1$ transitions to occur. Furthermore, $\Sigma^+ \rightarrow \Sigma^-$ transitions are rigidly forbidden. Therefore, when we pump the $A^2\Sigma^+(0,0^0,0)$ level, the only emission to the $(0,1,0)$ manifold which is observed is to the $X^2\Sigma^+(0,1^0,0)$ component.

*G. Herzberg, Molecular Spectra and Molecular Structure. III. Electronic Spectra of Polyatomic Molecules, Van Nostrand Reinhold, New York, pp. 20-37, 1966.

APPENDIX A.

VIBRATIONAL LEVEL TERMINOLOGY AND THE RENNER-TELLER EFFECT
IN LINEAR TRIATOMIC MOLECULES

13. (a) R.A. Copeland, D.R. Crosley, and G.P. Smith, "Laser-Induced Fluorescence Spectroscopy of NCO and NH₂ in Atmospheric Pressure Flames," submitted to the 20th Symposium (International) on Combustion, Ann Arbor, MI, August 1984. (b) D.R. Crosley, private communication.
14. R.A. Beyer and M.A. DeWilde, "Simple Burner for Laser Probing of Flames," Rev. Sci. Instrum., Vol. 53, p. 103, 1982. A description of the burner suitable for purposes of understanding the spectroscopy discussed in the present work is contained in Ref. 1.
15. Atomic line positions were obtained from G.R. Harrison, Massachusetts Institute of Technology Wavelength Tables, MIT, Cambridge, MA, 1969.
16. (a) J.A. Vanderhoff, R.A. Beyer, A.J. Kotlar, and W.R. Anderson, "Ar⁺ Laser Excited Fluorescence of C₂ and CN Produced in a Flame," Combustion and Flame, Vol. 49, p. 197, 1983. (b) K.N. Wong, J.A. Vanderhoff, W.R. Anderson, and A.J. Kotlar, to be published.
17. A.J. Kotlar, R.W. Field, J.I. Steinfeld, and J.A. Coxon, "Analysis of Perturbations in the A²Π - X²Σ⁺ "Red" System of CN," J. Mol. Spectrosc., Vol. 80, p. 86, 1980.
18. A.J. Kotlar, unpublished results.

REFERENCES

1. W.R. Anderson, J.A. Vanderhoff, A.J. Kotlar, M.A. DeWilde, and R.A. Beyer, "Intracavity Laser Excitation of NCO Fluorescence in an Atmospheric Pressure Flame," BRL Technical Report ARBRL-TR-02527, September 1983, A134740.
2. (a) R.A. Beyer, "Molecular Beam Sampling Mass Spectrometry of High Heating Rate Pyrolysis: Description of Data Acquisition System and Pyrolysis of HMX in a Polyurethane Binder," BRL Memorandum Report ARBRL-MR-02816, 1978, A054328. (b) C.U. Morgan and R.A. Beyer, "ESR and IR Spectroscopic Studies of HMX and RDX Thermal Decomposition," 15th JANNAF Combustion Meeting, Newport, RI, September 1978.
3. R.A. Fifer and H.E. Holmes, "Kinetics of the $\text{HCN} + \text{NO}_2$ Reaction Behind Shock Waves," J. Phys. Chem., Vol. 86, p. 2935, 1982.
4. R. Holland, D.W.G. Style, R.N. Dixon, and D.A. Ramsay, "Emission and Absorption Spectra of NCO and NCS," Nature (London), Vol. 182, p. 336, 1958.
5. R.N. Dixon, "The Absorption Spectrum of the Free NCO Radical," Phil. Trans. R. Soc. London, Vol. 252, p. 165, 1960.
6. P.S.H. Bolman, J.M. Brown, A. Carrington, I. Kopp, and D.A. Ramsay, "A Re-Investigation of the $\text{A}^2\Sigma^+ - \text{X}^2\Pi$ Band System of NCO," Proc. R. Soc. London Ser. A, Vol. 343, p. 17, 1975.
7. A. Carrington, A.R. Fabris, B.J. Howard, and N.J.D. Lucas, "Electron Resonance Studies of the Renner Effect. I. Gaseous NCO In Its $^2\Pi_{3/2}$ ($n=1$), $^2\Delta_{5/2}$ ($n=2$), and $^2\Phi_{7/2}$ ($n=3$) Vibronic States," Mol. Phys., Vol. 20, p. 961, 1971.
8. S. Saito and T. Amano, "Microwave Spectrum of the NCO Radical," J. Mol. Spectrosc., Vol. 34, p. 383, 1970.
9. T. Amano and E. Hirota, "Hyperfine Interactions of the Free NCO Radical in the Δ Vibronic State ($v_2=1$)," J. Chem. Phys., Vol. 57, p. 5608, 1972.
10. D.E. Milligan and M.E. Jacox, "Matrix Isolation Study of the Infrared and Ultraviolet Spectra of the Free Radical NCO," J. Chem. Phys., Vol. 47, p. 5157, 1967.
11. V.E. Bondybey and J.H. English, "Fermi Resonance and Vibrational Relaxation in the $\text{A}^2\Sigma$ State of NCO in Solid Argon," J. Chem. Phys., Vol. 67, p. 2868, 1977.
12. G.E. Barnes, J.M. Brown, A.D. Fackerell, and T.J. Sears, "The Laser Magnetic Resonance Spectrum of the NCO Radical at $5.2 \mu\text{m}$," J. Mol. Spectrosc., Vol. 92, p. 485, 1982.

ACKNOWLEDGEMENTS

K.N. Wong would like to express his gratitude to the Ballistic Research Laboratory and to the National Research Council for a postdoctoral fellowship. The authors would like to thank D.R. Crosley for a discussion of the results of Copeland, Crosley, and Smith prior to their publication, and T.J. Sears for a discussion of results in Reference 12.

stretching vibrations, about which little is currently known. Excited state spin relaxation, with retention of N^1 identity, is faster than electronic quenching by flame molecules.

The $(0,1^0,0)$ level involves one quantum of bending vibration in the 2Π ground state. Because of the Renner effect and spin-orbit splitting, there are four substates, $2\Sigma^+$, $2\Delta_{5/2}$, $2\Delta_{3/2}$, and $2\Sigma^-$, for this level.⁵ Since the upper state pumped by the laser is $2\Sigma^+$, one expects emission only to the $2\Sigma^+$ substate due to appropriate selection rules. For a $2\Sigma^+ - 2\Sigma^+$ transition, the selection rule $\Delta N = \pm 1$ holds, $\Delta N = 0$ being forbidden. Furthermore, the ground state spin splitting is larger than that of the excited state.⁵ Thus, one expects to observe doublet P and R branches. This is exactly what is observed in the $(0,1^0,0)$ emission band displayed in Figure 4. There is an extensive analysis of this band in Ref. 6 so that further analysis here would be superfluous. Using these results, the peaks at 4473.2 and 4473.9 Å are assigned as the R_{230} and R_{130} and those at 4482.8 and 4483.6 Å as the P_2 and P_1 heads, respectively. P_{232} and P_{132} are not resolved from their respective heads.

Information about excited state energy transfer can also be obtained from these spectra, as previously discussed.¹ As mentioned earlier, the Q_{131} and Q_{231} transitions have approximately equal intensities while R_{130} is about two times stronger than R_{230} (Figures 1-3). Now, the Q_1 , Q_2 , and R_1 branches all have unresolved satellites, namely, Q_{P21} , Q_{R12} , and Q_{R21} , respectively. One expects linestrengths of Q_1 and Q_2 to be nearly equal and stronger than Q_{P21} and Q_{R12} which are nearly equal. Calculations^{6,18} show the linestrengths of R_{230} , R_{130} , and R_{Q2130} all to be nearly equal. Therefore, comparison of either the Q-branch or the R-branch intensities indicates the laser produces approximately equal densities in the $N'=31$ spin components. This could occur via equal pumping rates of the two spin components. However, we have shown unambiguously that Q_{231} in the $(1,0^1,0)$ band is the pumping transition. Equal pump rates are not possible in this branch¹ because the Q_{231} and Q_{R1231} occur at nearly the same frequency and strongly overlap at 2500 K. Further, the Q_2 linestrength is about three times that of the Q_{R12} .^{6,18} Therefore, our earlier tentative interpretation that the molecule undergoes fast excited state spin relaxation with retention of N' identity in the flame is solidified. Furthermore, we point out that the spin relaxation rate must be much faster than electronic quenching. Otherwise, the nascent spin distribution excited by the laser would be frozen, since quenching would occur before spin redistribution.

IV. CONCLUSIONS

Laser excited fluorescence spectra of NCO in a $CH_4/N_2O/N_2$ flame have been observed using the 4658 Å line of an argon ion cw laser. Four bands were obtained as a result of emission from the $A^2\Sigma^+(0,0^0,0)$ level to different levels of the ground state. Three of the four bands display similar, 8-branch structures because they possess the same vibronic species in the upper and lower state, i.e., they are all $2\Sigma^+ \rightarrow 2\Pi$ transitions. The structure of the other band is considerably simpler because it is a $2\Sigma^+ \rightarrow 2\Sigma^+$ transition. All of the prominent lines in these bands originate from the $N'=31$ rotational level of the $A^2\Sigma^+(0,0^0,0)$ state. The region of the laser line, i.e., the $A^2\Sigma^+(0,0^0,0) \rightarrow X^2\Pi(1,0^1,0)$ transition, has been reinvestigated under improved experimental conditions and the previous Q_{231} pumping transition assignment is confirmed. Rotational analyses of the $(0,0^1,0)$, $(1,0^1,0)$, and $(0,0^1,1)$ emission bands have also been performed. The spin-orbit coupling constants and the rotational constants were obtained for these states. This analysis yields valuable information concerning the two ground state

TABLE 2. COMPARISON OF RESULTS OF ANALYSIS FOR SPECTRAL CONSTANTS (cm^{-1}) OF NCO

LEVEL	A" (SPIN-ORBIT PARAMETER)			B" (ROTATIONAL CONSTANT)		
$(0, 0^1, 0)$	-95.585 ^a	-95.6 ^b	-95.35 ± 0.44 ^c	0.38952 ^d	0.3895 ^b	0.3913 ± 0.0030 ^c
$(1, 0^1, 0)$	-----	-90.0 ^b	-90.17 ± 0.40 ^c	-----	0.3883 ^b	0.3892 ± 0.0027 ^c
$(0, 0^1, 1)$	-----	-97.3 ^b	-97.16 ± 0.13 ^c	0.38618 ^e	0.3861 ^b	0.3865 ± 0.0009 ^c

ν_1	-----	1275 ^f	1272 ^g	1272.0 ^b	1270.3 ± 2.7 ^c	
ν_3	1921.4 ^e	1922 ^f	1923 ^g	1922.5 ^b	1921.06 ± 0.89 ^c	
T_0	22754.06 ^a	-----	-----	-----	22755.3 ± 3.0 ^c	

a - Ref. 6

b - Ref. 13

c - This work. Error limits are one standard deviation.

d - Derived from microwave data^g, in Ref. 6. Rounded to five digits.

e - Ref. 12, rounded to five digits. B"_{0,0,1} is obtained by combining B"_{0,0,0} and α_3 . The value for ν_3 is increased by 0.8 cm^{-1} from the value 1920.6 cm^{-1} given in Ref. 12 (see text).

f - Ref. 10, Ar matrix results.

g - Ref. 11, Ar matrix results.

obtained from the fit to the $(0,0^1,0)$ data of Bolman, et al., was used and assumed to be the same for $(1,0^1,0)$ and $(0,0^1,1)$. (This value differs from that of Refs. 5 and 6, which may be ascribed to the presence of several higher order terms in the Hamiltonian used and to the fact that several of the constants of Bolman, et al. were obtained from other sources and fixed. All of the parameters in the present fit to the $(0,0^0,0)$ - $(0,0^1,0)$ band were allowed to vary.) Also, to insure that reliable values for G'' , A'' , and B'' could be obtained from a set of eight transitions having the same value of N' , the appropriate eight transitions were selected from the data of Bolman, et al., and were fitted in the same manner as the LEF data. The results for G'' , A'' , and B'' were within error limits of those from the fit of all the $(0,0^1,0)^{2\Sigma^+} - (0,0^0,0)^{2\Pi}$ band transitions and had rather small error limits. The experimental results for the $(0,0^1,0)$ band were next fitted. The results are shown in Table 2 and exhibit excellent agreement with Refs. 5 (not shown), 6, and 8 (though the error limits are larger, as expected, because of the moderate resolution and the small number of available lines).^{*} These results illustrate the validity of the technique. Finally, the $(1,0^1,0)$ and $(0,0^1,1)$ bands were fitted. For the $(1,0^1,0)$ band, the laser wavelength¹⁵ was used as the Q_{231} line position. Now, Q_2 branch line spacings near Q_{231} in the $(0,0^1,0)$ band are $\sim 1 \text{ cm}^{-1}$.^{5,6} One would expect similar spacings for this branch in the $(1,0^1,0)$ band. Thus, the laser line must be within $\sim 0.5 \text{ cm}^{-1}$ of Q_{231} in the $(1,0^1,0)$ band, or the laser would pump a different Q_2 line. As 0.5 cm^{-1} is the approximate precision limit of the measurements, it was deemed reasonable to use the laser line position in the fit. The standard deviations of the fits for the $(0,0^1,0)$, $(1,0^1,0)$, and $(0,0^1,1)$ bands were 0.60, 0.54, and 0.18 cm^{-1} , respectively. The constants are listed in Table 2.

There are a few things to point out about these results. First, Table 2 shows that the spin-orbit coupling constant changes significantly with different vibrations. Second, the values obtained for the $(0,0^1,1)$ emission band are much more precise than the rest, probably because of the extremely sharp and well-defined peaks of this band (Figure 3). Third, despite the moderate resolution used and the limited number of transitions, satisfactory results are obtained (see Table 2). For example, the constants obtained for the $(0,0^1,0)$ level agree with those determined with much higher resolution^{5,6,8} to within one standard deviation. Similarly, constants for the $(0,0^1,1)$ band agree with those from laser magnetic resonance (LMR) data¹² and from matrix studies.^{10,11} Note that v_3 from Ref. 12 is slightly smaller than it should be because the authors, having only LMR transitions in the $^{2\Pi_{3/2}}$ component available, were forced to use $A''_{0,0,0}$ from Ref. 6 in their analysis of the $(0,0^1,1)$ level. (This should not affect results for $B''_{0,0,1}$.) To first order, their result for v_3 , 1920.6 cm^{-1} , may be corrected by adding half of the difference in A'' values for the two levels, $\sim 0.8 \text{ cm}^{-1}$, to obtain 1921.4 cm^{-1} . Comparing our data with the preliminary results of Copeland, Crosley, and Smith,¹³ we see that the agreement is excellent except for v_3 . Gas phase constants for the $(1,0^1,0)$ level and for $A''_{0,0,1}$ have not previously been reported.

^{*}For argument's sake, we repeated this fit, but assumed $N'=30$ and then $N'=32$. The results did not agree with those of the earlier references at all.

Swan system fluorescence in this region also excited by the 4658Å line.¹⁶ However, the relative flame density profiles (Figure 11, Ref. 1) indicate that the concentration of C₂ drops much more quickly than that of NCO in the post-flame region. Thus, it is expected that in this region the concentration of NCO will increase relative to C₂. The best (1,0¹,0) spectrum that could be obtained in this manner is shown in Figure 2. It is seen that most of the C₂ peaks disappear (compare to Figure 9, Ref. 1) and the spectrum is amenable to analysis. A pair of strong peaks about the laser line are grating ghosts (determined experimentally by removing the flame). At the violet end of the band complications arise from unexpected lines. These complications may come from the (0,0⁰,0) 2Σ⁺ - (0,2¹,0) 2Π⁺ band, which appears because of a Fermi resonance between the (0,2¹,0) level and the (1,0¹,0) level.¹¹ In spite of these problems, features clearly analogous to those in Figures 1 and 3, namely P₂32, P₁32, Q₁31 (and their associated bandheads) and R₁30, are easily recognizable in Figure 2. In addition, small features assignable as the ⁰P₁₂33 (and associated bandhead), R₂30 and ⁵R₂₁29 are present. The only feature not present is the Q₂31, which is hidden by the intense laser scatter. The laser line position is centered between the two strong grating ghosts (see Figure 2). Clearly, the spacing of prominent lines is proper for assignment at this position as the Q₂31, unambiguously identifying this line as the pumping transition and confirming our previous tentative assignment.¹ No attempts were made to analyze lines from the (0,2¹,0) 2Π⁺ band.

The vibrational term value, G", the spin-orbit coupling constant, A", and the rotational constant, B", were determined for the (0,0¹,0), (1,0¹,0), and (0,0¹,1) levels of the ground state using the assigned transitions of the appropriate LEF spectra (Figures 1-3). A standard doublet Hamiltonian and weighted nonlinear least squares fitter¹⁷ were used to perform these calculations. Since the eight transitions available as input to the fitter for each of the three bands form a very small data set, and since each band has the same upper state, a separate determination of the A state constants was performed first. This was done by fitting the A²Σ⁺ (0,0⁰,0) - X²Π (0,0¹,0) data of Bolman, et al.,⁶ while allowing all the necessary upper and ground state constants to vary.¹⁸ The upper state constants thus obtained were held fixed for the subsequent calculations. The data from the LEF spectra were then fitted to determine the ground state constants G", A", and B". For these calculations, the lambda doubling parameters and centrifugal distortion constant, D", could not be determined from the data due to the moderate resolution of our apparatus. The lambda doubling parameters were set equal to zero while a value of D" = 3 x 10⁻⁷ cm⁻¹, the approximate value

¹⁶(a) J.A. Vanderhoff, R.A. Beyer, A.J. Kotlar, and W.R. Anderson, "Ar⁺ Laser Excited Fluorescence of C₂ and CN Produced in a Flame," Combustion and Flame, Vol. 49, p. 197, 1983. (b) K.N. Wong, J.A. Vanderhoff, W.R. Anderson, and A.J. Kotlar, to be published.

¹⁷A.J. Kotlar, R.W. Field, J.I. Steinfeld, and J.A. Coxen, "Analysis of Perturbations in the A²Σ⁺ - X²Π⁺ "Red" System of CN," J. Mol. Spectrosc., Vol. 80, p. 86, 1980.

¹⁸A.J. Kotlar, unpublished results.

TABLE 1. WAVELENGTHS (\AA) AND ASSIGNMENTS OF THE $(0,0^1,0)$, $(1,0^1,0)$,
AND $(0,0^1,1)$ EMISSION BANDS^a

$(0,0^1,0)$	$(1,0^1,0)$	$(0,0^1,1)$	Assignments
4408.99	4669.42		$0P_{12}$ head
4408.17	4668.92	4815.46	$0P_{12}33$
	4664.05	4810.50	$P_2 + {}^PQ_{12}$ head
4403.31	4663.51	4809.57	P_232
4398.36	4657.94 ^b	4803.89	Q_231
4393.75	4653.06	4798.47	R_230
			P_1 head
4388.92	4648.56	4792.02	P_131
			$Q_1 + {}^Qp_{21}$ head
4384.69	4643.90	4787.97	
4383.98	4642.92	4786.29	Q_131
4379.18	4637.75	4780.78	R_130
4374.94	4632.69	4775.46	$S_{R_21}29$

a - Table entries between two assignments indicate overlapped lines.

b - Argon laser wavelength from Ref. 15.

P_2 , and $0P_{12}$ branch prominent lines. All of the expected eight prominent lines from $N'=31$ and four associated bandheads appear in each of the $2\Sigma^+ - 2\Pi$ vibrational bands (except for the one obscured by laser scatter). Note the strikingly similar features of these spectra. For example, in all three bands, R_130 is about two times stronger than R_230 whereas Q_131 and Q_231 are of similar intensities. In the $(1,0^1,0)$ band shown in Figure 2, the shoulder at 4632.69\AA has been assigned as the $S_{R_21}29$ instead of the larger peak at 4633.17\AA , based on rotational line spacing considerations. This is the only assignment which gives a reasonable fit in our rotational analysis (vide infra).

In our previous work, the region of the laser line at 4658\AA was investigated in order to identify the rotational transition pumped by this line. Although evidence suggested that the Q_2 branch line is pumped, the assignment was not firm because of interferences from grating ghosts and C_2

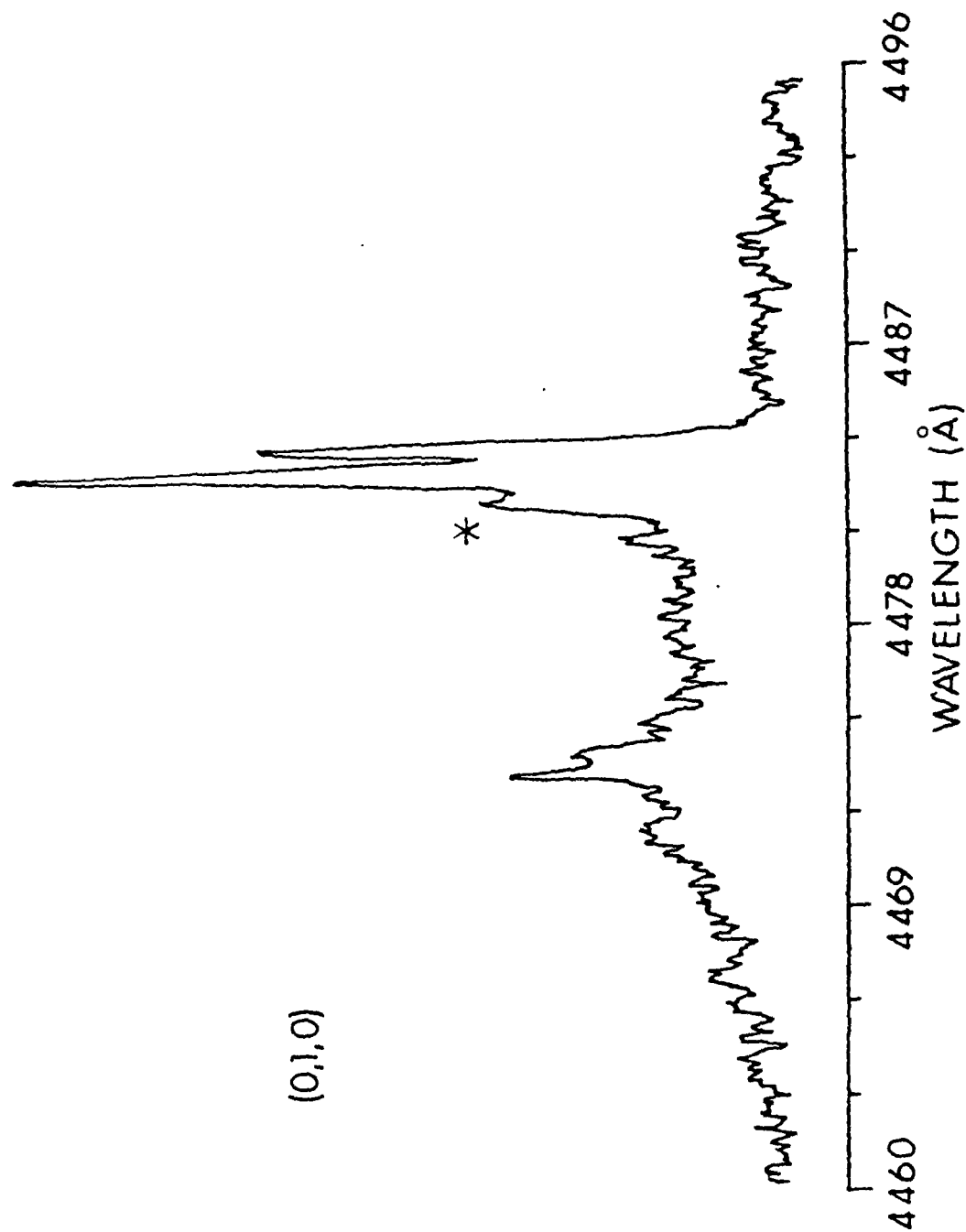


Figure 4. The $A^2\Sigma^+(0,0^0,0) + X^2\Sigma^+(0,1^0,0)$ Fluorescence Spectrum

DISTRIBUTION LIST

<u>No. Of Copies</u>	<u>Organization</u>	<u>No. Of Copies</u>	<u>Organization</u>
1	Superintendent Naval Postgraduate School Dept. of Aeronautics ATTN: D.W. Netzer Monterey, CA 93940	2	Atlantic Research Corp. ATTN: M.K. King 5390 Cherokee Avenue Alexandria, VA 22314
5	AFRPL (DRSC) ATTN: R. Geisler D. George D Weaver J. Levine W. Roe Edward AFB, CA 93523	1	Atlantic Research Corp. ATTN: R.H.W. Waesche 7511 Wellington Road Gainesville, VA 22065
1	Air Force Armament Laboratory ATTN: AFATL/DLODL Eglin AFB, FL 32542	1	AVCO Everett Rsch. Lab. Div. ATTN: D. Stickler 2385 Revere Beach Parkway Everett, MA 02149
2	AFOSR ATTN: L.H. Caveny J.M. Tishkoff Bolling Air Force Base Washington, DC 20332	1	Battelle Memorial Institute Tactical Technology Center ATTN: J. Huggins 505 King Avenue Columbus, OH 43201
1	AFWL/SUL Kirtland AFB, NM 87117	2	Exxon Research & Eng. Co. ATTN: A. Dean M. Chou P.O. Box 45 Linden, NJ 07036
1	NASA Langley Research Center ATTN: G.B. Northam/MS 168 Hampton, VA 23365	1	Ford Aerospace and Communications Corp. DIVAD Division Div. Hq., Irvine ATTN: D. Williams Main Street & Ford Road Newport Beach, CA 92663
4	National Bureau of Standards ATTN: J. Hastie M. Jacox T. Kashiwagi H. Semerjian US Department of Commerce Washington, DC 20234	1	General Electric Armament & Electrical Systems ATTN: M.J. Bulman Lakeside Avenue Burlington, VT 05401
1	Aerojet Solid Propulsion Co. ATTN: P. Micheli Sacramento, CA 95813	1	General Electric Company ATTN: M. Lapp Schenectady, NY 12301
1	Applied Combustion Technology, Inc. ATTN: A.M. Varney P.O. Box 17885 Orlando, FL 32860	1	Air Force Armament Laboratory ATTN: AFATL/DLODL Eglin AFB, FL 32542-5000

DISTRIBUTION LIST

<u>No. Of Copies</u>	<u>Organization</u>	<u>No. Of Copies</u>	<u>Organization</u>
1	General Motors Rsch Labs Physics Department ATTN: R. Teets Warren, MI 48090	1	Los Alamos National Lab ATTN: B. Nichols T7, MS-B284 P.O. Box 1663 Los Alamos, NM 87545
3	Hercules, Inc. Alleghany Ballistics Lab. ATTN: R.R. Miller P.O. Box 210 Cumberland, MD 21501	1	Olin Corporation Smokeless Powder Operations ATTN: R.L. Cook P.O. Box 222 St. Marks, FL 32355
3	Hercules, Inc. Bacchus Works ATTN: K.P. McCarty P.O. Box 98 Magna, UT 84044	1	Paul Gough Associates, Inc. ATTN: P.S. Gough 1048 South Street Portsmouth, NH 03801
1	Hercules, Inc. AFATL/DL DL ATTN: R.L. Simmons Eglin AFB, FL 32542	2	Princeton Combustion Research Laboratories, Inc. ATTN: M. Summerfield N.A. Messina 475 US Highway One Monmouth Junction, NJ 08852
1	Honeywell, Inc. Defense Systems Division ATTN: D.E. Broden/ MS MN50-2000 600 2nd Street NE Hopkins, MN 55343	1	Hughes Aircraft Company ATTN: T.E. Ward 8433 Falbrook Avenue Canoga Park, CA 91303
1	IBM Corporation ATTN: A.C. Tam Research Division 5600 Cottle Road San Jose, CA 95193	1	Rockwell International Corp. Rocketdyne Division ATTN: J.E. Flanagan/HB02 6633 Canoga Avenue Canoga Park, CA 91304
1	Director Lawrence Livermore National Laboratory ATTN: C. Westbrook Livermore, CA 94550	3	Sandia National Laboratory Combustion Sciences Dept. ATTN: R. Cattolica D. Stephenson P. Mattern Livermore, CA 94550
1	Lockheed Missiles & Space Co. ATTN: George Lo 3251 Hanover Street Dept. 52-35/B204/2 Palo Alto, CA 94304	1	Sandia National Laboratory ATTN: M. Smooke Division 8353 Livermore, CA 94550
		1	Science Applications, Inc. ATTN: R.B. Edelman 23146 Cumorah Crest Woodland Hills, CA 91364

DISTRIBUTION LIST

<u>No. Of Copies</u>	<u>Organization</u>	<u>No. Of Copies</u>	<u>Organization</u>
1	Science Applications, Inc. ATTN: H.S. Pergament 1100 State Road, Bldg. N Princeton, NJ 08540	2	United Technologies Corp. ATTN: R.S. Brown R.O. McLaren P.O. Box 358 Sunnyvale, CA 94086
1	United Technologies ATTN: A.C. Eckbreth East Hartford, CT 06108	1	Universal Propulsion Company ATTN: H.J. McSpadden Black Canyon Stage 1 Box 1140 Phoenix, AZ 85029
4	SRI International ATTN: S. Barker D. Crosley D. Golden Tech Lib 333 Ravenswood Avenue Menlo Park, CA 94025	1	Veritay Technology, Inc. ATTN: E.B. Fisher P.O. Box 22 Bowmansville, NY 14026
1	Stevens Institute of Tech. Davidson Laboratory ATTN: R. McAlevy, III Hoboken, NJ 07030	1	Brigham Young University Dept. of Chemical Engineering ATTN: M.W. Beckstead Provo, UT 84601
1	Teledyne McCormack-Selph ATTN: C. Leveritt 3601 Union Road Hollister, CA 95023	1	California Institute of Tech. Jet Propulsion Laboratory ATTN: MS 125/159 4800 Oak Grove Drive Pasadena, CA 91103
1	Thiokol Corporation Elkton Division ATTN: W.N. Brundige P.O. Box 241 Elkton, MD 21921	1	California Institute of Technology ATTN: F.E.C. Culick/ MC 301-46 204 Karman Lab. Pasadena, CA 91125
3	Thiokol Corporation Huntsville Division ATTN: D.A. Flanagan Huntsville, AL 35807	1	University of California, Berkeley Mechanical Engineering Dept. ATTN: J. Daily Berkeley, CA 94720
3	Thiokol Corporation Wasatch Division ATTN: J.A. Peterson P.O. Box 524 Brigham City, UT 84302	1	University of California Los Alamos National Lab. ATTN: T.D. Butler P.O. Box 1663, Mail Stop B216 Los Alamos, NM 87545

DISTRIBUTION LIST

<u>No. Of Copies</u>	<u>Organization</u>	<u>No. Of Copies</u>	<u>Organization</u>
2	University of California, Santa Barbara Quantum Institute ATTN: K. Schofield M. Steinberg Santa Barbara, CA 93106	1	University of Illinois Dept. of Mech.-Indust Engr. ATTN: H. Krier 144MEB, 1206 W. Green St. Urbana, IL 61801
1	University of Southern California Dept. of Chemistry ATTN: S. Benson Los Angeles, CA 90007	1	Johns Hopkins University/APL Chemical Propulsion Information Agency ATTN: T.W. Christian Johns Hopkins Road Laurel, MD 20707
1	Case Western Reserve Univ. Div. of Aerospace Sciences ATTN: J. Tien Cleveland, OH 44135	1	University of Minnesota Dept. of Mechanical Engineering ATTN: E. Fletcher Minneapolis, MN 55455
1	Cornell University Department of Chemistry ATTN: E. Grant Baker Laboratory Ithaca, NY 14853	4	Pennsylvania State University Applied Research Laboratory ATTN: G.M. Faeth K.K. Kuo H. Palmer M. Micci University Park, PA 16802
1	Univ. of Dayton Rsch Inst. ATTN: D. Campbell AFRPL/PAP Stop 24 Edwards AFB, CA 93523	1	Polytechnic Institute of NY ATTN: S. Lederman Route 110 Farmingdale, NY 11735
1	University of Florida Dept. of Chemistry ATTN: J. Winefordner Gainesville, FL 32611	2	Princeton University Forrestal Campus Library ATTN: K. Brezinsky I. Glassman P.O. Box 710 Princeton, NJ 08540
3	Georgia Institute of Technology School of Aerospace Engineering ATTN: E. Price Atlanta, GA 30332	1	Princeton University MAE Dept. ATTN: F.A. Williams Princeton, NJ 08544
2	Georgia Institute of Technology School of Aerospace Engineering ATTN: W.C. Strahle B.T. Zinn Atlanta, GA 30332		

DISTRIBUTION LIST

<u>No. Of Copies</u>	<u>Organization</u>	<u>No. Of Copies</u>	<u>Organization</u>
2	Purdue University School of Aeronautics and Astronautics ATTN: R. Glick J.R. Osborn Grissom Hall West Lafayette, IN 47962		<u>Aberdeen Proving Ground</u> Dir, USAMSAA ATTN: AMXSY-D AMXSY-MP, H. Cohen Cdr, USATECOM ATTN: AMSTE-TO-F Cdr, CRDC, AMCCOM ATTN: SMCCR-RSP-A SMCCR-MU SMCCR-SPS-IL
3	Purdue University School of Mechanical Engineering ATTN: N.M. Laurendeau S.N.B. Murthy D. Sweeney TSPC Chaffee Hall West Lafayette, IN 47906		
1	Rensselaer Polytechnic Inst. Dept. of Chemical Engineering ATTN: A. Fontijn Troy, NY 12181		
2	Southwest Research Institute ATTN: R.E. White A.B. Wenzel 8500 Culebra Road San Antonio, TX 78228		
1	Stanford University Dept. of Mechanical Engineering ATTN: R. Hanson Stanford, CA 94305		
1	University of Texas Dept. of Chemistry ATTN: W. Gardiner Austin, TX 78712		
1	University of Utah Dept. of Chemical Engineering ATTN: G. Flandro Salt Lake City, UT 84112		
1	Virginia Polytechnic Institute and State University ATTN: J.A. Schetz Blacksburg, VA 24061		

USER EVALUATION SHEET/CHANGE OF ADDRESS

This Laboratory undertakes a continuing effort to improve the quality of the reports it publishes. Your comments/answers to the items/questions below will aid us in our efforts.

1. BRL Report Number _____ Date of Report _____
2. Date Report Received _____
3. Does this report satisfy a need? (Comment on purpose, related project, or other area of interest for which the report will be used.) _____

4. How specifically, is the report being used? (Information source, design data, procedure, source of ideas, etc.) _____

5. Has the information in this report led to any quantitative savings as far as man-hours or dollars saved, operating costs avoided or efficiencies achieved, etc? If so, please elaborate. _____

6. General Comments. What do you think should be changed to improve future reports? (Indicate changes to organization, technical content, format, etc.) _____

CURRENT
ADDRESS

Name

Organization

Address

City, State, Zip

7. If indicating a Change of Address or Address Correction, please provide the New or Correct Address in Block 6 above and the Old or Incorrect address below.

OLD
ADDRESS

Name

Organization

Address

City, State, Zip

(Remove this sheet along the perforation, fold as indicated, staple or tape closed, and mail.)

----- FOLD HERE -----

Director
US Army Ballistic Research Laboratory
ATTN: AMXBR-OD-ST
Aberdeen Proving Ground, MD 21005-5066

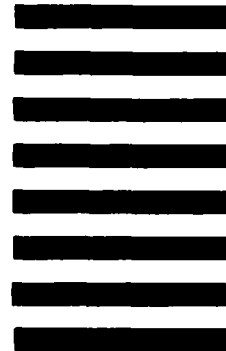


NO POSTAGE
NECESSARY
IF MAILED
IN THE
UNITED STATES

OFFICIAL BUSINESS
PENALTY FOR PRIVATE USE, \$300

BUSINESS REPLY MAIL
FIRST CLASS PERMIT NO 12062 WASHINGTON, DC
POSTAGE WILL BE PAID BY DEPARTMENT OF THE ARMY

Director
US Army Ballistic Research Laboratory
ATTN: AMXBR-OD-ST
Aberdeen Proving Ground, MD 21005-9989



----- FOLD HERE -----

END

FILMED

6-85

DTIC